*Journal of Applied Fluid Mechanics*, Vol. 8, No. 4, pp. 863-870, 2015.
Available online at www.jafmonline.net, ISSN 1735-3572, EISSN 1735-3645.
DOI: 10.18869/acadpub.jafm.73.238.23311

# Applications of Shallow Water SPH Model in Mountainous Rivers

R. Chen[1], S. Shao[1,2], X. Liu[1] and X. Zhou[1†]

[1] *State Key Laboratory of Hydraulics and Mountain River Engineering, Sichuan University, Chengdu 610065, China*
[2] *Department of Civil and Structural Engineering, University of Sheffield, Sheffield S1 3JD, UK (Visiting University, Beijing)*

†*Corresponding Author Email: xiaoquan_zhou@126.com*

(Received June 7, 2014; accepted July 4, 2014)

## ABSTRACT

In this paper, the Shallow Water Equations (SWEs) are solved by the Smoothed Particle Hydrodynamics (SPH) approach. The proposed SWE-SPH model employs a novel prediction/correction two-step solution algorithm to satisfy the equation of continuity. The concept of buffer layer is used to generate the fluid particles at the inflow boundary. The model is first applied to several benchmark water flow applications involving relatively large bed slope that is typical of the mountainous regions. The numerical SWE-SPH computations realistically disclosed the fundamental flow patterns. Coupled with a sediment morph-dynamic model, the SWE-SPH is then further applied to the movement of sediment bed load in an L-shape channel and a river confluence, which demonstrated its robust capacity to simulate the natural rivers.

**Keywords**: SWE; SPH; Two-step solution; Prediction/correction; Sediment transport; Buffer layer; Mountainous region.

## 1. INTRODUCTION

Most areas in the southwest region of China are located in the mountainous regions. Numerous natural hazards such as the landslide initiated by the earthquake and the storm rain can block the natural river and as these rivers are located over complicated mountainous topographies with relatively large bed slope, disastrous flooding can unpredictably occur involving large water surface variations and cause damages of property and losses of life to the local residents. Thus the study of these mountainous flows has both theoretical and practical significance.

Numerical models provide an effective approach to study a wide range of such flooding flows due to their economic costs and good efficiencies to predict the flow under different conditions without the need of large physical space and heavy labor work. For example, Xia et al. (2010) combined the hydrodynamic and sediment models and studied the dam break flows over a mobile bed. Other good numerical work has also been done by Mehdizadeh et al. (2008) and Souza et al. (2010). However, most traditional numerical methods are based on the Eulerian grid approach and solved by the FDM/FEM/FVM schemes. These kinds of approach can meet serious issues when they are applied to the flows over mountainous region due to the critical requirement imposed by the treatment of advection term in the Navier-Stokes equations and the dry/wet boundaries.

The Smoothed Particle Hydrodynamics (SPH) is a pure mesh-free numerical technique and its potentials to the hydrodynamic applications are fully explored by Monaghan (1992). SPH is a Lagrangian particle method that does not require the grid to evaluate the spatial derivatives. It is a quite simple but robust technique to treat the large deformation of free surfaces and multi-interfaces. A number of researchers have successfully applied the SPH to complicated benchmark physics as evidenced in Liu and Liu (2003). Until now, two kinds of SPH solution algorithms are widely used in the coastal and river hydraulics, i.e. weakly compressible SPH and incompressible SPH, depending on the different pressure solution techniques. Also most SPH simulations are carried out in the vertical 2D plane and the full Navier-Stokes equations have also been solved by SPH.

Quite recently the SPH solutions of the Shallow Water Equations (SWEs) are gaining increasing attention. This is due to the fact that most natural flow hazards happen over a relatively large space and the practical interest is to interpret these flow characteristics in the horizontal plane rather than the detailed information along the flow depth. In this

sense, the vertical 2D or 3D SPH solutions based on the Navier-Stokes equations are computationally very demanding. Thus the SPH solutions of SWEs are expected to provide a more robust tool in view of the practical engineering interest. Since the concept of SWE-SPH was originally proposed by Wang and Shen (1999) in 1D dam break flow, it has been successfully applied in more complicated 2D dam break flows (De Leffe et al., 2010), open channel flows (Chang and Chang, 2013) and flooding simulations (Vacondio et al., 2012). Most existing SWE-SPH solutions are based on the variational approach proposed by Rodriguez-Paz and Bonet (2005) and adopted a one-step solution algorithm, that is to say, the particle columns are advected to their next positions using a single-step time integration. Thus the numerical scheme is fully explicit. In this sense, computational time steps must be strictly controlled to maintain the computational stability and accuracy. To improve the numerical performance of the SWE-SPH, which finds its potentials in practical engineering fields, in this work we will propose a two-step prediction/correction solution scheme for the SWE-SPH, similar to the two-step semi-implicit incompressible SPH solutions of Shao and Lo (2003), although the nature of numerical scheme is still explicit. The advantage of this new SWE-SPH solution algorithm is that slightly larger time steps can be used, as the continuity of the fluid system is imposed at the second step. Generally speaking, the overall computational efficiency has been improved.

To tentatively test the proposed SWE-SPH model in horizontal 2D flows, the model is first applied to two benchmark water flow applications, including the dam break flow passing over a horizontal rectangular channel and through a steep U-shaped channel. Then by further combining with the sediment morph-dynamic equations, the sediment bed load movement and bed deformation are investigated for an L-shape channel as well as a mobile bed river confluence. All of the tests are carried out under relatively larger bed slopes to represent the practical mountainous river bathymetries. Although only qualitative validations and analysis are carried out, the model applications indicated that the proposed SWE-SPH can provide a promising solution technique for the simulation of flows over large and complicated areas.

## 2. GOVERNING EQUATIONS

The fundamental principles of the SWE-SPH model are to represent the fluid system as discrete particle columns, in comparison with the circular shape of particles used in a vertical 2D or 3D SPH framework. The proposed SWE-SPH is based on a 2-D plan projection of the domain, in which the flow velocity through the height of vertical column is uniform and the instantaneous spatial variation of the column height is small. Following this, in a SPH discretisation of the resulting 2-D plan domain, each particle represents a column of fluid of a certain height. The continuum is discretised with a system of Lagrangian particles, in which each particle represents a column of water of height $h$ with constant mass $m$, which moves over the computational domain. The unknowns of the problem are the spatial positions of every particle column at each time step and the height of the water column.

Thus the continuity and momentum equations are represented in the following forms as:

$$\frac{dh}{dt} + h\nabla \cdot \mathbf{u} = 0 \tag{1}$$

$$\frac{d\mathbf{u}}{dt} = -g(\nabla h + \nabla z) - \frac{n^2 |\mathbf{u}|}{h^{4/3}}\mathbf{u} \tag{2}$$

where $h$ = flow depth or height of particle column; $t$ = time; $\mathbf{u}$ = horizontal velocity vector; $g$ = gravitational acceleration; $z$ = bed elevation; and $n$ = roughness of bed.

To further consider the fact that the channel bottom is composed by a sediment layer whose characteristic is given by $z_b(x, y, t)$ laying on a non-erodible foundation (Jaan et al., 2014), the sediment motion due to the bed load transport can be modeled by the following morph-dynamic formulation as:

$$\frac{\partial z_b}{\partial t} + \xi \frac{\partial q_{bx}}{\partial x} + \xi \frac{\partial q_{by}}{\partial y} = 0 \tag{3}$$

where $\xi = 1/(1-n)$ and $n$ = porosity of sediment layer; $q_{bx}$ and $q_{by}$ represent the sediment transport rate, which depends on the local hydraulic conditions.

Most of the bed load transport formulas relate the bed load transport rate with the flow shear stress. However, an alternative approach, the Grass formula, which simply links the bed load transport to the flow velocities, has been adopted in many sediment transport models due to its simplicity and effectiveness. Another distinctive advantage of this formula is that in an engineering river, velocity measurement is much more readily available than the shear stress. For these reasons, it is also used in present work:

$$q_{bx} = Au(u^2 + v^2)^{\frac{m-1}{2}} \tag{4}$$

$$q_{by} = Av(u^2 + v^2)^{\frac{m-1}{2}} \tag{5}$$

where $A$ and $m$ are the empirical parameters determined by the properties of sediment grain; $u$ and $v$ = two velocity components.

## 3. TWO STEP SOLUTION METHOD

The SPH concept has been widely used in coastal hydrodynamics in recent years and thus the basic principles are not interpreted here. More detailed information can be found in Monaghan (1992) and Liu and Liu (2003). In the framework of SPH algorithms, the interpolation and first derivative

operators of a variable $f(x_I)$ can be represented in a general way as:

$$f(\mathbf{x}_I) = \sum_{J=1}^{N} V_j(\mathbf{x}_J) f(\mathbf{x}_J) W_{IJ} \tag{6}$$

$$\nabla f(\mathbf{x}_I) = \sum_{J=1}^{N} V_j(\mathbf{x}_J) f(\mathbf{x}_J) \nabla W_{IJ} \tag{7}$$

where $I$ and $J$ indicate the reference and neighboring particle columns, respectively; $\mathbf{x}$ = particle column position; $V$ = volume of particle column; and $W$ = SPH kernel function represented by

$$W(a,r) = \frac{0.4547}{r^2} \begin{cases} 1 - \frac{3}{2}\left(\frac{a}{r}\right)^2 + \frac{3}{4}\left(\frac{a}{r}\right)^3 & 0 < \frac{a}{r} < 1 \\ \frac{1}{4}\left(2 - \left(\frac{a}{r}\right)\right)^3 & 1 \le \frac{a}{r} \le 2 \\ 0 & \frac{a}{r} > 2 \end{cases} \tag{8}$$

where $a/r$ = relative distance between two particle columns.

The two-step SWE-SPH solution procedures are carried out as follows:

***Step 1:*** This is the so-called prediction approach, in which only the topographical and bed resistance forces in Equation (2) are used and temporary particle column velocity and position are obtained as

$$\mathbf{u}^* = \mathbf{u}^n + \Delta t \left( -g\nabla z - \frac{n^2 |\mathbf{u}|}{h^{4/3}} \mathbf{u} \right)^n \tag{9}$$

$$\mathbf{X}^* = \mathbf{X}^n + \frac{\left(\mathbf{u}^n + \mathbf{u}^*\right)}{2} \Delta t \tag{10}$$

where superscript $n$ and $^*$ refer to the previous and intermediate time step values, respectively; and $\Delta t$ = time step.

***Step 2:*** This is the so-called correction step, in which the corrected particle column height $h$ is used to update the intermediate column velocities and positions computed from Equations (9) - (10). This process satisfies the fluid incompressibility condition that is similar to the two-step ISPH solution method of Shao and Lo (2003). The procedure follows:

$$\mathbf{u}^{n+1} = \mathbf{u}^* + (-g\nabla h)\Delta t \tag{11}$$

$$\mathbf{X}^{n+1} = \mathbf{X}^* + \frac{\left(\mathbf{u}^{n+1} + \mathbf{u}^n\right)}{2} \Delta t \tag{12}$$

where $n+1$ refers to the new time step values.

***Step 3***: This is actually the computational procedure between Step 1 and 2. The updated flow depth $h$ to correct the particle column velocity and position is derived from the mass conservation or fluid continuity as represented in Equation (1), which can also be conceptually represented as

$$hr^2 = const = h_0 r_0^2 \tag{13}$$

where $h_0$ and $r_0$ are the original particle column height and influence radius at the beginning of the computation, which can be evaluated from the initial particle arrangement. During the computation we will have

$$r_I = r_0 \left( \frac{h_0}{h_I} \right)^{0.5} \tag{14}$$

where $h_I = \sum_J h_J r_J^2 W_I(a_J, r_I)$ is an implicit function and can only be solved through the iterative method as below:

$$R\left(h_I^{(k)}\right) = h_I^{(k)} - \sum_J h_J r_J^2 W_I\left(a_J, r_I^{(k)}\right) \tag{15}$$

where $R(h_I^{(k)})$ is the residual of $k^{th}$ iteration and the next iteration is carried out as

$$h_I^{(k+1)} = \sum_J h_J r_J^2 W_I\left(a_J, r_I\left(h_I^{(k)}\right)\right) \tag{16}$$

$$r_I^{(k)} = r_I^0 \left( \frac{h_I^0}{h_I^{(k)}} \right)^{0.5} \tag{17}$$

Finally, the column height is updated by the following

$$h_I^{(k+1)} = h_I^{(k)} - \frac{R_I^{(k)}}{\left(\frac{dR}{dh}\right)_I^{(k)}}$$

$$= h_I^{(k)} \left( 1 - \frac{R_I^{(k)}}{\left( h_I - \sum_J h_J r_J^2 W_I - \sum_J \frac{h_J r_J^2}{2} a_{IJ} \frac{dW_I}{da_{IJ}} \right)^{(k)}} \right)$$

$$= h_I^{(k)} \left( 1 - \frac{2R_I^{(k)}}{2R_I^{(k)} - \sum_J h_J r_J^2 a_{IJ} \frac{dW_I}{da_{IJ}}} \right) \tag{18}$$

The above process is repeated, until the solution of the computed water column height is converged.

In the above SWE-SPH computations, the time step should satisfy the stability criterion as imposed by the so-called Courant condition as

$$\Delta t \le C_{FL} \frac{r_I}{\sqrt{g h_I} + |\mathbf{u}_I|} \tag{19}$$

which implies that the particle column movement within a certain time step should be a fraction of the influence radius under the actions of flow velocity and wave celerity.

According to Rodriguez-Paz and Bonet (2005), the coefficient $C_{FL}$ is generally less than 10% in their test cases. By using the proposed semi-implicit SWE-SPH solution scheme in this work we found it can be as large as 50%.

## 4. BOUNDARY TREATMENT

The following shallow water boundary conditions

are used in the SWE-SPH model.

**Upstream inflow boundaries:** A buffer zone is used to treat the inflow open boundary, in which three layers of the particles are arranged: The first row of velocity particles, the second row of pressure correction particles and the third row of buffer particles. The first row of particles ensures the correct flow input rate into the computational domain and the second row reduces the numerical dissipation of flow velocity at the inflow boundary, while the third row prevents the numerical noise arising from the addition of new particles and acts as a buffer zone for the interpolation. A schematic setup of the inflow zone particles is shown in Fig. 1 and the SPH computed uniform flow at the inlet boundary is compared with the FLUENT result in Fig. 2. This shows the proposed inflow boundary treatment works well.

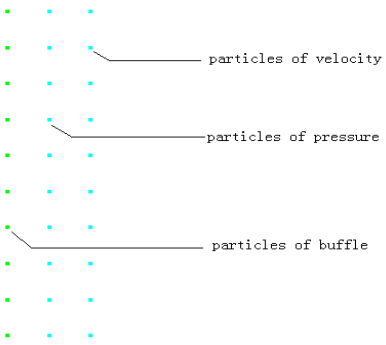


**Fig. 1. Treatment of inflow boundary using three layers of particle.**

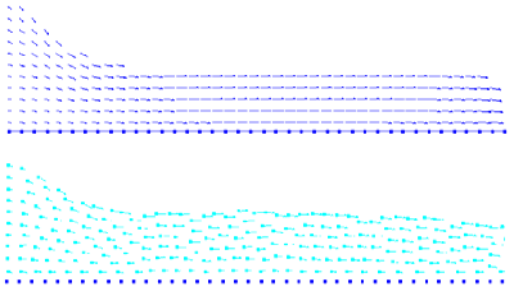

**Fig. 2. Uniform inflow computed by SWE-SPH and FLUENT (upper: SWE-SPH; lower: FLUENT).**

**Moving dry/wet boundaries:** A major advantage of the SPH approach over the classic finite volume or finite difference method in the shallow water flow simulation is due to its automatic treatment of the moving boundary conditions following the particle column movement. Thus no additional algorithm is needed to track the edge of dry/wet boundaries.

**Solid walls:** Special treatment must be made near the vicinity of solid walls in order for the motion of the adjacent fluids to be modeled correctly. The wall boundary conditions in SPH can be modeled either by the fixed dummy particles (Koshizuka et al., 1998) or moving mirror particles (Cummins and Rudman, 1999). In this work, the former is used for the simplicity of the algorithm.

## 5. SWE-SPH MODEL TEST IN WATER FLOWS

In this section, the proposed SWE-SPH model is applied to two benchmark flow tests, i.e. dam break flows over a horizontal bed and through a U-shaped channel over relatively steep slope.

### 5.1 Dam Break Flow Over a Horizontal Bed

An ideal rectangular channel that is 6 m long and 1 m wide is horizontally placed as shown in Fig. 3. The roughness of the channel bed is $n$ = 0.01. The initial water reservoir is 2 m long and the upstream and downstream water levels are 1.0 m and 0.0 m, respectively. The dam break is assumed to happen instantaneously.

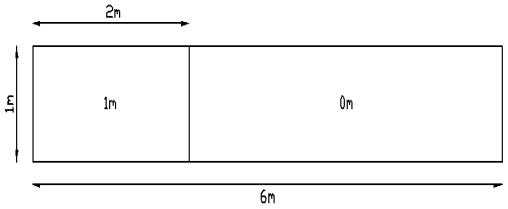


**Fig. 3. Schematic setup of dam break flow over a horizontal bed.**

Following the SWE-SPH numerical simulations, the computed particle snapshots and free surface profiles at time $t$ = 0.4 s after the dam break are shown in Fig. 4 (a) and (b), respectively. As a comparison, the analytical solutions of SWE and the numerical results from vertical 2D SPH (Shao and Lo, 2003) are also shown in Fig. 4 (b). It shows that the SWE-SPH results matched the analytical solutions very well but there are some disagreements with the 2D SPH computations. This is because the latter was based on the solutions of fully incompressible Navier-Stokes equations and the propagation speed of pressure wave is infinite. In contrast, in the SWE-SPH modeling, the pressure wave propagates in a finite speed depending on the flow depth. As a result, the vertical 2D SPH predicted a faster free surface propagation with lower surface height. It is not surprising that the SWE-SPH computations closely matched the analytical solutions, as both ignored the vertical variations of flow variables and averaged the flow parameters along the depth.

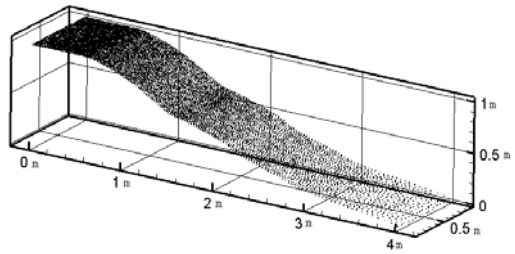


**Fig. 4 (a). SWE-SPH computed particle snapshots of dam break flow at time $t$ = 0.4 s.**

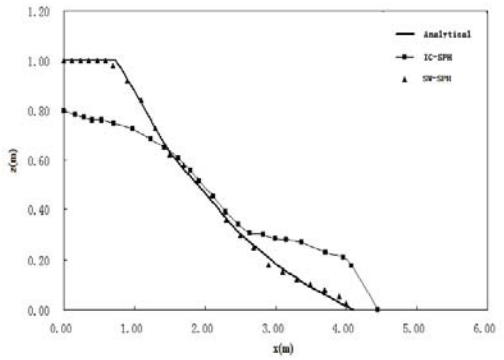


**Fig. 4.(b). SWE-SPH (SW-SPH) computed water surface profiles, compared with vertical 2D SPH (IC-SPH) results and analytical solutions.**

## 5.2 Dam Break Flow in an U-shaped Channel

In this test, a dam break flow occurs in an U-shaped channel that is 5 m long for both the upstream and downstream sections and 1 m wide. The radius of the inner and outer circular bend is 1 m and 2 m, respectively. The bed slope of the channel is 0.01 and roughness is 0.0136. It is assumed three cylinders are located inside the channel each with a radius of 0.1 m. The inflow discharge is 0.2 $m^3/s$ and the free outflow condition is imposed at the downstream outlet.

Following the SWE-SPH computations, the dam break flow velocity fields at time $t$ = 3.0 s and 9.0 s are shown in Fig. 5. It is shown that as the flows interact with the cylinder barriers, the free surfaces are elevated and the disturbances are generated to propagate in the upstream direction in the form of disturbance wave.

In addition, the particle snapshots and locally enlarged velocity fields near the cylinder at time $t$ = 21 s are shown in Fig. 6, which also demonstrated that the unstable flow patterns are produced behind the barrier and the complicated flow circulations are observed.

## 6. SWE-SPH MODEL TEST IN SEDIMENT FLOWS

To further test the SWE-SPH model capacity to compute the movable bed sediment transport in an L-shaped channel with pre-arranged sediment layers, the numerical test reported by Castro Diaz et al. (2009) is used. The detailed computational setups including the initial and boundary conditions can be found in the original work of Castro Diaz et al. (2009).

So this is not repeated here. According to their recordings, the water density is 1000 $kg/m^3$, the sediment density 2600 $kg/m^3$ and sediment grain size 0.001 m. The Manning's coefficient is 0.0196, the non-dimensional critical shear stress 0.047 and sediment porosity 0.4.

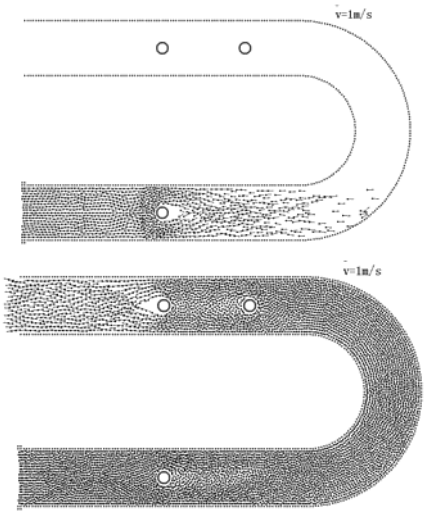


**Fig. 5. SWE-SPH computed flow velocity field in U-shape channel at $t$ = 3.0 s (upper) and 9.0 s (lower).**

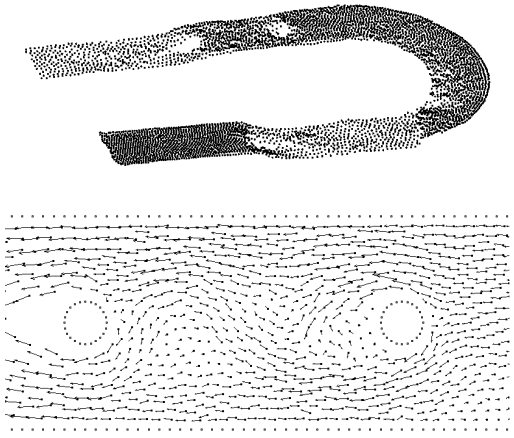

**Fig. 6. SWE-SPH computed particle snapshot (upper) and local velocity field (lower) in U-shape channel at $t$ = 21 s.**

Following the SWE-SPH computations, the evolution of the sediment layers in the L-shaped channel is shown in Fig. 7, at time $t$ = 400 s, 900 s and 1200 s, respectively.

It is shown that the computed sediment bed evolutions are generally consistent with the Finite Volume solutions of Castro Diaz et al. (2009), especially the maximum erosion location and amplitude are adequately captured. To initially validate this, the FVM result of Castro Diaz et al. (2009) at time $t$ = 900 s is shown in Fig. 7 (d) for a comparison. It is observed that the main erosion area concentrates near the region within $X$ = (2, 4) and $Y$ = (0, 1).

Here it should be mentioned that Castro Diaz et al. (2009) used the Meyer-Peter formula for sediment transport in their model while the Grass model is used in present study.

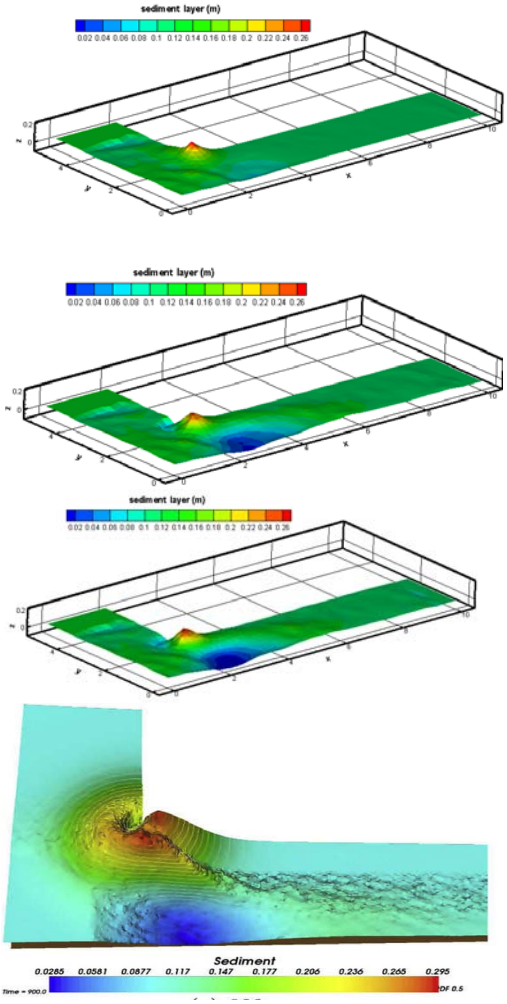


**Fig. 7. SWE-SPH computed sediment bed evolutions at $t$ = 400 s (first), 900 s (second), 1200 s (third), compared with FVM solutions of Castro Diaz et al. (2009) at $t$ = 900 s (last figure).**

## 7. SWE-SPH MODEL APPLICATION IN CASE STUDY

The channel confluences are widely found in hydraulic engineering fields. A large number of studies have found that the dynamics of open-channel flow at river confluences depend on the channel geometry and flow parameters such as the cross-sectional area, bed slope, angle of river junction, discharge ratio, downstream Froude number and hydraulic roughness, etc. In the numerical simulations, two-dimensional flow models that take into account the flows in the main and transverse directions have been widely used in the last decade. Examples of different hydraulic models for studying the complex river flow configurations can be found in Biron et al. (2002) and Duan and Nanda (2006). However, the flow and sediment motions at the river confluence and in the main river considering the tributary effect are very complicated, especially in case of the torrential river confluence. Here we will apply the proposed SWE-SPH scheme to simulate the flow and sediment transport in a torrential river confluence caused by the upstream dam break.

The study area belongs to a tributary of the Liusha River, which is a typical mountainous river with steep bed slope. Natural disasters due to the torrential river confluence are often reported which caused damages of property and losses of life. Quite a few field investigations and numerical simulations have been carried out in this river and its tributaries in order to understand the flow regimes. A schematic view of the simulation area is shown in Fig. 8. The main river inlet flow discharge is 136.5 $m^3/s$ and its bed slope is 0.02. The tributary river inlet flow discharge is 24.5 $m^3/s$ and its bed slope is 0.04. The free outflow boundary condition is imposed at the downstream outlet. The water density is 1000 $kg/m^3$, sediment density 2600 $kg/m^3$, sediment porosity 0.4, Manning's coefficient 0.014 and CFL parameter 0.5.

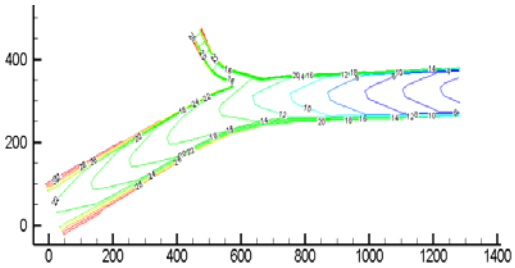


**Fig. 8. Simulation area of river confluence in Liusha River tributary**

According to the local hydrological station survey, the sediment properties in this area are shown in Table 1 as blow:

**Table 1 Sediment gradation distributions**

| Sediment gradation distributions (mm) | | | | | | | | |
|---|---|---|---|---|---|---|---|---|
| Gravel | | | Shingle | | Sand | | | |
| >60 | 60~40 | 40~20 | 20~10 | 10~2 | 2~0.5 | 0.5~0.25 | 0.25~0.075 | 0.075~0.005 |
| % | % | % | % | % | % | % | % | % |
| | 15.5 | 38.5 | 20 | 14 | 8 | 2 | 1.5 | 0.5 |

Based on the SWE-SPH computations, the flow velocity fields and sediment bed load transports are shown in Figs. 9 and 10 (a) – (d), respectively, at different time instants at $t$ = 20 s, 40 s, 80 s and 120 s. Fig. 9 shows that due to the relatively steep bed slope of the river channel, the upstream dam break flow demonstrates the characteristics of large flow velocity and shallow water depth, i.e. 2.5 ~ 3.5 m/s above. It is also observed that the tributary river entered the main flow with high speed and the flow path generated a meandering pattern. After the two rivers converged, the flow velocity further increased to over 4.5 m/s in the main flow. The SWE-SPH simulations realistically disclosed the flow patterns which are difficult to deal with by the traditional grid methods due to frequent variations of the wet/dry boundary and difficult tasks to treat the advection term. Also, the SWE-SPH effectively reduced the computational load as only the area covered by the particles was considered in the simulation.

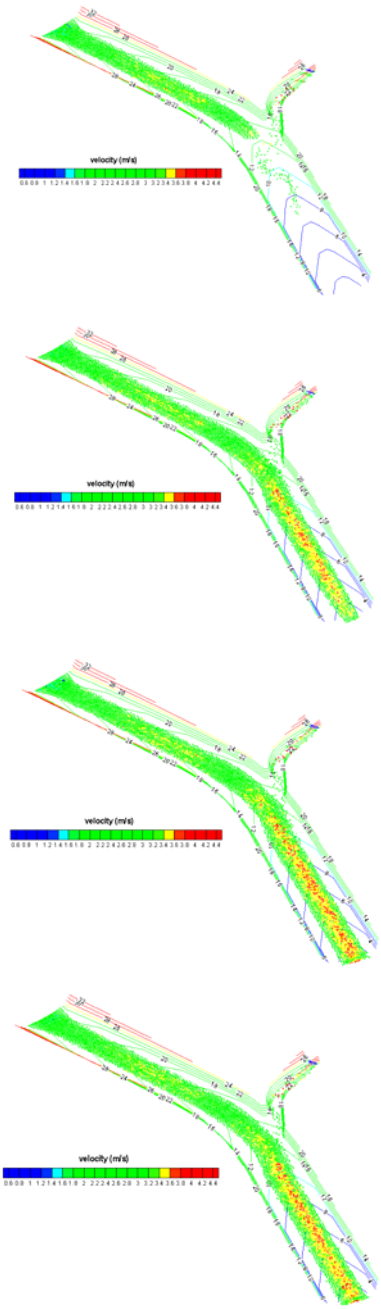


**Fig. 9. SWE-SPH computed flow velocity contours of river confluence at time $t$ (a) 20 s, (b) 40 s, (c) 80 s and (d) 120 s (from up to down).**

Further examining the corresponding sediment transport patterns as shown in Fig. 10, it shows that the sediment transport rate is high where the flow velocity is high. When the flow velocity is small, there is almost no sediment bed load transport. One important phenomenon disclosed is that significant sediment movement is produced downstream of the river confluence where the two flows converge and it is concluded that the river bed should undergo severe erosions in this section, which should be given adequate attention in the engineering practice and effective measures should be taken to protect the river bed. The capacity of SWE-SPH to simulate practical mountainous rivers is fully demonstrated.

Figs. 9 and 10 also indicate that the flow and sediment motions nearly reach the equilibrium stage as there is almost no obvious difference observed between the last two figures at time $t$ = 80 s and 120 s.

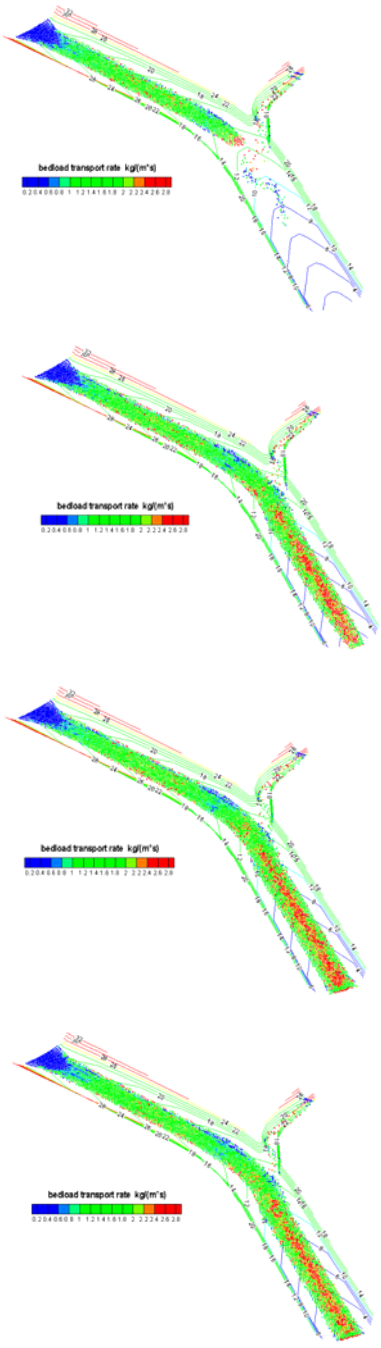


**Fig. 10. SWE-SPH computed sediment transport contours of river confluence at time $t$ (a) 20 s, (b) 40 s, (c) 80 s and (d) 120 s (from up to down).**

## 8. CONCLUSIONS

In this paper, we have presented a shallow water SPH formulation for the simulation of dam break flows and sediment bed load transport in mountainous rivers. The proposed model, which is

based on the two-step solution method, is able to simulate many kinds of shallow water cases which are commonly found in the engineering applications. The simulation results indicated that the numerical technique is robust and accurate to disclose useful flow and sediment information. Although only qualitative validations have been carried out, the proposed SWE-SPH algorithms could provide a promising trend to develop the next generation of simple and effective SPH models for practical interest. All of the computations in this study were finished within several minutes by using dual U9600 CPU 1.6G and RAM 3G laptop computer.

## ACKNOWLEDGEMENTS

This research work is supported by the Start-up Grant for Young Teachers of Sichuan University (2014SCU11056) and the National Science and Technology Support Plan (2012BAB0513B0).

## REFERENCES

Biron, P. M., A. Richer, A. D. Kirkbride, A. G. Roy and S. Han (2002). Spatial patterns of water surface topography at a river confluence. *Earth Surface Processes and Landforms* 27, 913–928.

Castro Diaz, M. J., E. D. Fernandez-Nieto, A. M. Ferreiro and C. Pares (2009). Two-dimensional sediment transport models in shallow water equations: A second order finite volume approach on unstructured meshes. *Comput. Methods Appl. Mech. Eng.* 198, 2520–2538.

Chang, T. J. and K. H. Chang (2013). SPH modeling of one-dimensional nonrectangular and nonprismatic channel flows with open boundaries. *Journal of Hydraulic Engineering ASCE*, 139(11), 1142-1149.

Cummins, S. J. and M. Rudman (1999). An SPH projection method. *Journal of Computational Physics* 152(2), 584-607.

De Leffe, M., D. Le Touze and B. Alessandrini (2010). SPH modeling of shallow-water coastal flows. *Journal of Hydraulic Research* 48, 118–125.

Duan, J. G. and S. K. Nanda (2006). Two dimensional depth averaged model simulation of suspended sediment concentration distribution in a groyne field. *Journal of Hydrology* 327, 426–437.

Koshizuka, S., A. Nobe and Y. Oka (1998). Numerical analysis of breaking waves using the moving particle semi-implicit method. *Int. J. Numer. Meth. Fluids* 26, 751-769.

Liu, G. R. and M. B. Liu (2003). *Smoothed Particle Hydrodynamics: A Meshfree Particle Method.* World Scientific.

Mehdizadeh, A., B. Firoozabadi and B. Farhanieh (2008). Numerical simulation of turbidity current using $\overline{v^2} - f$ turbulence model. *Journal of Applied Fluid Mechanics* 1, 45-55.

Monaghan, J. J. (1992). Smoothed particle hydrodynamics. *Annu Rev Astron Astrophys* 30, 543–74.

Pu, J. H., K. Hussain, S. D. Shao and Y. F. Huang (2014). Shallow sediment transport flow computation using time-varying sediment adaptation length. *International Journal of Sediment Research* 29, 135-147.

Rodriguez-Paz, M. and J. Bonet (2005). A corrected smooth particle hydrodynamics formulation of the shallow-water equations. *Computers and Structures*, 83, 1396–1410.

Shao, S. D. and E. Y. M. Lo (2003). Incompressible SPH method for simulating Newtonian and non-Newtonian flows with a free surface. *Advances in Water Resources* 26, 787–800.

Souza, L. B. S., H. E., Schulz, S. M. Villela and J. S. Gulliver (2010). Experimental study and numerical simulation of sediment transport in a shallow reservoir. *Journal of Applied Fluid Mechanics* 3, 9-21.

Vacondio, R., B. D. Rogers and P. K. Stansby (2012). Accurate particle splitting for smoothed particle hydrodynamics in shallow water with shock capturing. *Int. J. Numer. Meth. Fluids* 69, 1377–1410.

Wang, Z. L. and H. T. Shen (1999). Lagrangian simulation of one–dimensional dam-break flow. *Journal of Hydraulic Engineering, ASCE*, 125(11), 1217-1220.

Xia, J., B. Lin, R. Falconer and G. Wang (2010). Modelling dam-break flows over mobile beds using a 2D coupled approach. *Advances in Water Resources* 33, 171–183